Computers, Materials & Continua
DOI: 10.32604/cmc.2022.030447
Article

Tech Science Press

Transfer Learning for Chest X-rays Diagnosis Using Dipper Throated Algorithm

Hussah Nasser AlEisa[1], El-Sayed M. El-kenawy[2,3], Amel Ali Alhussan[1,*], Mohamed Saber[4], Abdelaziz A. Abdelhamid[5,6] and Doaa Sami Khafaga[1]

[1]Department of Computer Sciences, College of Computer and Information Sciences, Princess Nourah Bint Abdulrahman University, Riyadh, 11671, Saudi Arabia
[2]Department of Communications and Electronics, Delta Higher Institute of Engineering and Technology, Mansoura, 35111, Egypt
[3]Faculty of Artificial Intelligence, Delta University for Science and Technology, Mansoura, 35712, Egypt
[4]Electronics and Communications Engineering Department, Faculty of Engineering, Delta University for Science and Technology, Mansoura, 35712, Egypt
[5]Department of Computer Science, Faculty of Computer and Information Sciences, Ain Shams University, Cairo, 11566, Egypt
[6]Department of Computer Science, College of Computing and Information Technology, Shaqra University, 11961, Saudi Arabia
*Corresponding Author: Amel Ali Alhussan. Email: aaalhussan@pnu.edu.sa
Received: 26 March 2022; Accepted: 26 April 2022

Abstract: Most children and elderly people worldwide die from pneumonia, which is a contagious illness that causes lung ulcers. For diagnosing pneumonia from chest X-ray images, many deep learning models have been put forth. The goal of this research is to develop an effective and strong approach for detecting and categorizing pneumonia cases. By varying the deep learning approach, three pre-trained models, GoogLeNet, ResNet18, and DenseNet121, are employed in this research to extract the main features of pneumonia and normal cases. In addition, the binary dipper throated optimization (DTO) algorithm is utilized to select the most significant features, which are then fed to the K-nearest neighbor (KNN) classifier for getting the final classification decision. To guarantee the best performance of KNN, its main parameter (K) is optimized using the continuous DTO algorithm. To test the proposed approach, six evaluation metrics were employed namely, positive and negative predictive values, accuracy, specificity, sensitivity, and F1-score. Moreover, the proposed approach is compared with other traditional approaches, and the findings confirmed the superiority of the proposed approach in terms of all the evaluation metrics. The minimum accuracy achieved by the proposed approach is (98.5%), and the maximum accuracy is (99.8%) when different test cases are included in the evaluation experiments.

Keywords: Metaheuristic; pneumonia; dipper throated optimization; KNN

1 Introduction

In children under the age of five, pneumonia damages the lungs and is responsible for 18% of all fatalities [1]. In addition, two billion people throughout the globe suffer yearly from pneumonia infections, and death might ensue if it is not detected and treated early. Pneumonia should be diagnosed as soon as possible. Rapid diagnosis using chest X-rays performed by a skilled radiologist is thus necessary to prevent misdiagnosis. An X-ray of the chest is the most frequent and cost-effective approach to diagnose pneumonia [2,3]. The lack of radiologist professionals, particularly in low-resource nations and rural areas, leads to lengthy delays for diagnosis, which in turn raises the mortality rate. It is difficult to make a definitive diagnosis of pneumonia using chest X-ray pictures since several conditions with similar symptoms and appearances, such as opacity, cavities, and pleural effusions might be misdiagnosed as pneumococcal illness. The detection of illnesses by using chest X-rays is thus hampered. Researchers have proposed a variety of technologies and computer-aided diagnostic (CAD) tools for X-ray image processing that enable radiologists to identify distinct types of chest X-ray pneumonia [4,5]. Many biological problems have been addressed using a combination of handcrafted and machine learning methods, as well as deep learning and machine learning. Recent advances in the approach of artificial intelligence (AI) I and machine learning, deep learning exploit multi-layered artificial neural networks in a wide range of applications, including voice recognition and language translation. Deep learning approaches for machine learning may learn representations from data such as videos, photos, and text without explicitly coding rules or depending on direct human intervention. With their versatility and capacity to draw inferences from data, they are able to increase their forecast accuracy by supplying more information [6,7].

In this paper, a novel approach is proposed for classifying the pneumonia cases robustly. The proposed approach is based on extracting a set of features from the given X-ray images using transfer learning of three strong deep learning architectures, namely, GoogLeNet, ResNet18, and DenseNet121. The extracted features are then processed to select only the most significant features that enable the K-nearest neighbor (KNN) classifier to achieve the best performance. To guarantee the best performance of KNN, its parameter is optimized using the dipper throated optimization algorithm. To check the superiority of the proposed approach, several experiments were conducted to compare the performance of the proposed approach with the other approaches. The achieved findings confirm the superiority of the proposed approach.

The remainder of this paper is structured as follows. A review of the recently published research is included in Section 2. Information on the algorithms employed to develop the proposed approach is provided in Section 3. Section 4 illustrates the structure of the suggested methodology. The findings and achieved results are given in Section 5. The conclusions and plans for future research are discussed in Section 6.

2 Related Works

Pneumonia may be detected on chest X-ray pictures utilizing a number of approaches that have been published in the scientific literature. Some of these systems rely on handmade feature extraction techniques, while others depend on deep learning algorithms for extracting robust features and categorization [8–10]. The parameters of deep layered convolutional neural networks (CNNs) for pneumonia diagnosis have been altered by these approaches, allowing for higher illness detection accuracy via the usage of these models. As a baseline model, the researchers in [11–14] utilized logistic regression to identify patients with pneumonia by analyzing X-ray images. Using logistic regression, the area under the curve (AUC) yields unsatisfactory results. They were able to improve their results by using a set of dense layers in a convolutional network (DenseNet). The network was honed with the aid of Adam optimizer. According to the model's AUC, it is possible to diagnose pneumonia with an accuracy of (60.9%), which is slightly higher than that of logistic regression (60%).

An accurate model for diagnosing pneumonia was developed by the researchers in [15] and is referred to as ChexNet. One of the most important features of ChexNet is the 121-layer CNN that analyzes and classifies the X-ray images then locates them using a thermal map. Pneumonia may be difficult to be diagnosed; thus, the model's findings were compared against those of four radiologists using F1. In comparison to the typical radiologist, the ChexNet model achieved an F1-score of (0.435). On the other hand, mask-RCNN and a residual network were implemented by the authors in [16–20]. In order to identify pneumonia, it was employed to construct a computer-aided detection system. Overfitting was remedied by using residual mapping in the residual network. Batch normalization was utilized after each activation and convolution. Binary cross-entropy for the loss function and Intersection over Union were then combined (IoU). A pooling block was utilized to reduce the number of arguments. A bounding box was utilized to locate items in the Mask Regional CNN. The RPN and RoI-align were the two steps of the process. Extracting features was accomplished by using a bottom-up and top-down extraction strategy based on the feature pyramid network (FPN). Mask-RCNN had an accuracy of (78.06%) with a confidence level of (98%), whereas a confidence level of (70%) is achieved by the residual network.

A dropout layer-based and a dropout-free CNN architecture were introduced in [21–25]. Convolution, maximum pooling, and classification layers were all included in both CNNs. The feature extractor was separated into two portions by a sequence of convolution and maximum pooling layers. Each of the 32×32 convolution layers has a maximum pooling layer of 3×3 in size, and an activation function of type rectified linear unit (ReLU) in the first section. As well as the ReLU activator and the maximum pooling layer of size 2×2, the second section contains two convolution layers of 64 and 128 units [26–31]. ReLU is a well-known activation function in neural networks, particularly in CNNs. Nonlinearity was introduced into the model using the ReLU layer. It was discovered that three standard deep learning approaches based on CNNs could successfully categorize pneumonia and normal cases based on chest X-ray pictures [32–38]. These models are GoogLeNet, ResNet18, and DenseNet121. We found that ResNet-18 performed better than the other two. Tab. 1 summarizes the literature models and their findings.

Table 1: Recent studies addressing the application of CNN in identifying pneumonia cases

Paper	Approach	Precision	AUC	Recall	F1-score	Accuracy
[1]	ResNet18, AlexNet, SqueezeNet, DenseNet201	97%	98%	99%	98.1%	98%
[12]	DenseNet121	-	60.9%	-	-	-
[13]	DensNet121	-	-	-	43.5%	-
[15]	CNN	-	71.7%	90.7%	-	78.9%
[16]	(deep ResNet), mask RCNN + FPN + Adam	-	-	51.52%	-	85.60%
[17]	Mask R-CNN, RetinaNet	61.1%	-	83.5%	-	26.2%

(Continued)

Table 1: Continued

Paper	Approach	Precision	AUC	Recall	F1-score	Accuracy
[18]	Mask R-CNN, RetinaNet + FPN	75.8%	-	79.3%	77.5%	-
[19]	CNN	-	-	-	-	90.68%

3 Basic Algorithms

In this section, the main algorithms employed in this research are introduced. These algorithms include deep learning for extracting the main features from the input images of the pneumonia cases. In addition, they employed a feature selection algorithm for selecting the significant features. Moreover, the classification of the pneumonia cases is performed in terms of the KNN algorithm, which is optimized using one of the recent parameters optimization algorithms in the literature. The following section briefly introduces each one of these algorithms.

3.1 Deep Learning

An increasing number of clinical diagnostic and medical image applications are relying on deep learning, and one such application is that of CNNs, which are types of multi-layer neural networks specifically designed for the identification of visual patterns in pixel images with little or no prior processing. Many advantages come from using CNNs, including the capacity to extract more relevant information from pictures than can be done manually. Several CNN-based deep networks have been suggested by computer vision researchers to segment images, classify images, recognize objects, and pinpoint their locations inside images. Along with tackling natural computer vision issues, CNNs have shown to be very effective at identifying diseases including Alzheimer's disease and breast cancer, as well as detecting and classifying skin blemishes.

Deep learning in medical image analysis has also been discussed in depth. In this research, we adopted a set of deep learning models for feature extraction; these models are GoogLeNet, ResNet18, and DenseNet121. In specific, we selected the features from the most promising model. Based on our findings that ResNet18 is the best performing model, the features are extracted mainly in terms of this model. The basic building block of ResNet18 is depicted in Fig. 1. The models consist of multiple units of this building block. The building block consists of two chunks of 3×3 convolutional layers with a relu activation function.

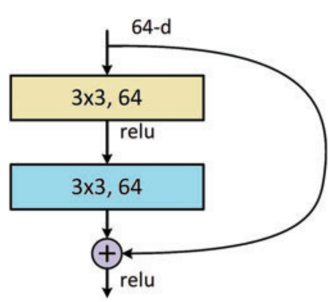

Figure 1: The building block for ResNet18

3.2 Feature Selection

Pattern categorization, machine learning, information retrieval, data analysis, and data mining all depend mainly on feature selection. While the approach works well for a dataset with few characteristics, classification operations employing multiple features were not included in this method's assessment. There may be the need for additional approaches like those provided by the feature selection if the dataset has a large number of characteristics, such as thousands. Fig. 2 illustrates this. There are two variables involved in classification using FS: an input variable that represents all of the data and a final output that represents the classification pattern based on features that were previously picked.

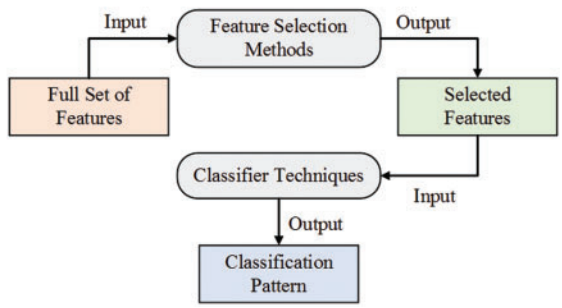

Figure 2: Feature selection for classification tasks

3.3 KNN Algorithm

The most straightforward technique for pattern recognition is the KNN algorithm, which has been frequently employed in the literature as an easy-to-understand supervised classifier. By taking into account their K closest neighbor samples in train data, the KNN classifies any sample of test data. In a K-neighbor network, the samples belong to whichever cluster has the most significant number of fellow members. The KNN classifier has two parameters: the distance calculation technique and the number of K. SEN, SPE, and ACC are all metrics used to gauge the classifier's effectiveness. PPV and NPV are used to estimate the classifier's ability to predict outcomes accurately. Assuming that two features are retrieved from an input test sample, the binary KNN classification method is shown in Fig. 3.

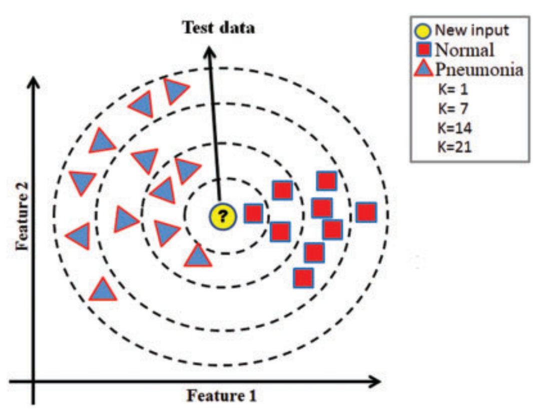

Figure 3: Illustration of the KNN classifier

Algorithm 1: The DTO Algorithm

Initialization positions $P_i (i = 1, 2, \ldots, n)$ with size n,
velocities $V_i (i = 1, 2, \ldots, n)$, total number of iterations T_{max},
fitness function f_n, c, C_1, C_2, C_3, C_4, C_5, r_1, r_2, R, $t = 1$
Calculate objective function f_n for each bird BP_i
Find best bird P_{best}
  While $t \leq Tmax$ **do**
    for $(i = 1 \ : i < n + 1)$ **do**
      if $(R < 0.5)$ **then**
        Update position of current swimming bird as
        $P_{nd}(t+1) = P_{best}(t) - C_1.|C_2.P_{best}(t) - P_{nd}(t)|$
      else
        Update velocity of current flying bird as
        $V(t+1) = C_3 V(t) + C_4 r_2 (P_{best}(t) - P_{nd}(t)) + C_5 r_2 (P_{Gbest} - P_{nd}(t))$
        Update position of current flying bird as
        $P_{nd}(t+1) = P_{nd}(t) + V(t+1)$
      end if
    end for
  Calculate objective function f_n for each bird P_i
  Update c, C_1, C_2, R
  Find best bird P_{best}
  Set $P_{Gbest} = P_{best}$
  Set $t = t + 1$
Return best bird P_{Gbest}

3.4 Parameter Optimization

To achieve better performance of the classification models in machine learning, careful choice of the model parameters is an essential step, as the model performance depends mainly on the values of these parameters. The manual or random selection of these parameters cannot guarantee better performance. In addition, the trial-and-error method is usually time-consuming to reach the best parameters. In this case, the optimization algorithms are the best alternative to help researchers find the best set of parameters necessary for a machine learning model to achieve better performance. In the literature, many optimizers can perform this task. In this research, we adopted the recently published dripper throated optimization (DTO) algorithm for optimizing the K parameter of the KNN classification algorithm. The detailed steps of the DTO algorithm are presented in Algorithm 1. This algorithm is based on three matrices, namely positions (P), Velocities (V), and fitness function f, defined in the following.

$$P = \begin{bmatrix} P_{1,1} & P_{1,2} & P_{1,3} & \ldots & P_{1,d} \\ P_{2,1} & P_{2,2} & P_{2,3} & \ldots & P_{2,d} \\ P_{3,1} & P_{3,2} & P_{3,3} & \ldots & P_{3,d} \\ \ldots & \ldots & \ldots & \ldots & \ldots \\ P_{m,1} & P_{m,2} & P_{m,3} & \ldots & P_{m,d} \end{bmatrix} \quad (1)$$

$$V = \begin{bmatrix} V_{1,1} & V_{1,2} & V_{1,3} & \dots & V_{1,d} \\ V_{2,1} & V_{2,2} & V_{2,3} & \dots & V_{2,d} \\ V_{3,1} & V_{3,2} & V_{3,3} & \dots & V_{3,d} \\ \dots & \dots & \dots & \dots & \dots \\ V_{m,1} & V_{m,2} & V_{m,3} & \dots & V_{m,d} \end{bmatrix} \tag{2}$$

$$f = \begin{bmatrix} f_1\left(P_{1,1}, P_{1,2}, P_{1,3}, \dots, P_{1,d}\right) \\ f_2\left(P_{2,1}, P_{2,2}, P_{2,3}, \dots, P_{2,d}\right) \\ f_3\left(P_{3,1}, P_{3,2}, P_{3,3}, \dots, P_{3,d}\right) \\ \dots \\ f_m\left(P_{m,1}, P_{m,2}, P_{m,3}, \dots, P_{m,d}\right) \end{bmatrix} \tag{3}$$

where the position and velocity of the i^{th} bird in the j^{th} dimension is denoted by $P_{i,j}$ and $V_{i,j}$ for $i \in 1, 2, 3, \dots, m$ and $j \in 1, 2, 3, \dots, d$. For each bird, the values of the fitness functions $f = f_1, f_2, f_3, \dots, f_n$ are used to find the best values of locations and speed of each bird, which is used to find the best solution. For more details on the DTO algorithm, please refer to [39].

4 The Proposed Methodology

The structure of the proposed system is depicted in Fig. 4. As shown in the figure, the process starts with collecting X-ray images from X-ray machines and then sending them to the machine learning blocks, based on a set of algorithms implemented to classify the input X-ray images as normal for pneumonia cases. The processing included in the machine learning block starts with preprocessing and augmentation, followed by the proposed approach. The details of the proposed approach are depicted in Fig. 5. More information on these steps is presented and discussed in the following sections.

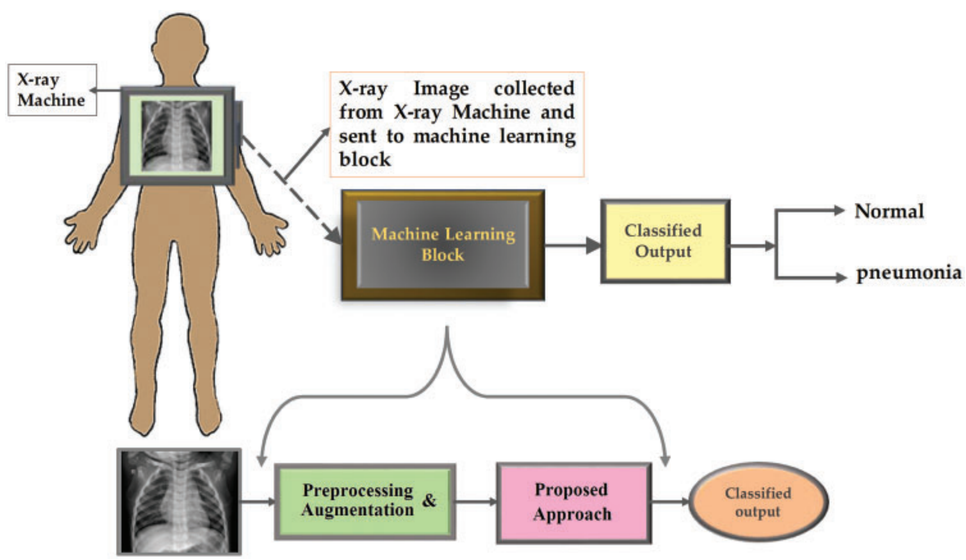

Figure 4: The structure of the proposed methodology

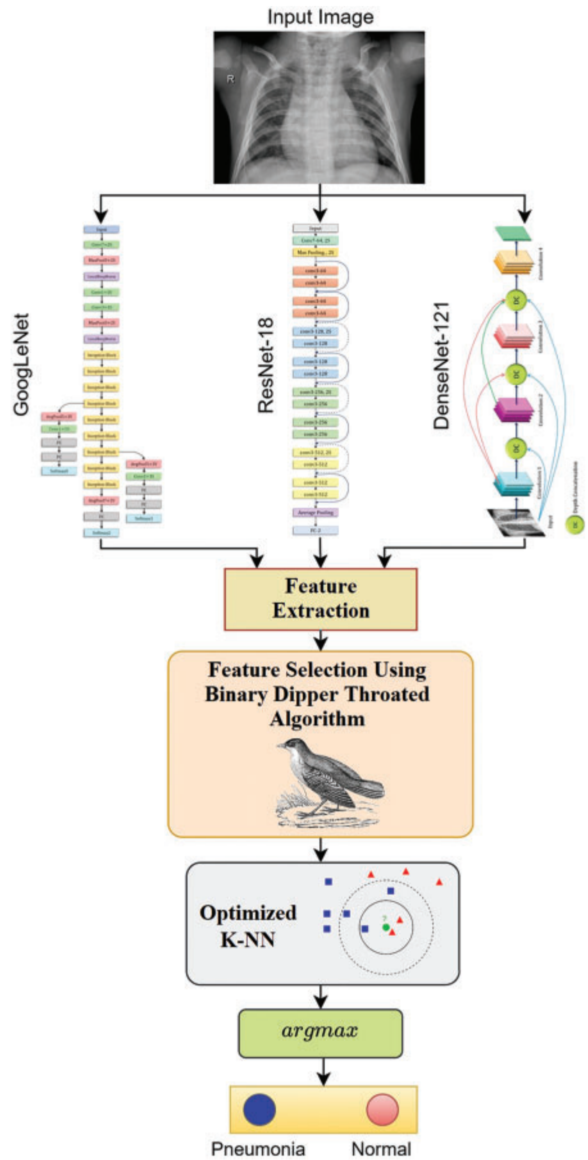

Figure 5: The detailed steps of the proposed methodology

4.1 Dataset

The pneumonia images utilized in this research were taken from Kaggle's pneumonia dataset, which contains 5247 images with resolutions between 400 and 2000 pixels [36]. Tab. 2 shows that 3906 of the 5247 chest X-ray pictures (2561 bacterial and 1345 viral) were taken from patients with pneumonia, while 1341 images were taken from healthy people. Some cases of pneumonia are caused by a combination of bacterial and viral infections. Even though viral and bacterial co-infections are not included in the dataset utilized in this research. In this research, we considered viral and bacterial pneumonia as one set referred to as pneumonia. Therefore, we have only two classes in our classification task, namely, normal case and pneumonia case. Fig. 6 presents samples of the images in the employed dataset.

Table 2: Details of the pneumonia dataset

Type	Number of images
Pneumonia (Bacterial)	2561
Pneumonia (Viral)	1345
Normal	1341
Total	5247

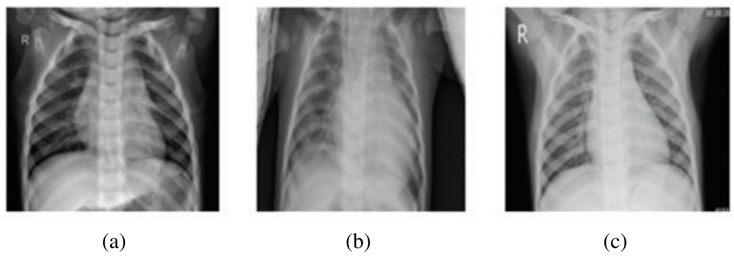

Figure 6: Sample images from the Kaggle dataset (a) Normal case, (b) Pneumonia (Bacteria) case, and (c) Pneumonia (Viral) case

4.2 Preprocessing & Augmentation

The dataset images are preprocessed to improve the results of the later steps of the proposed approach. Resizing the input images in the dataset is the first step that is applied to make the images fit the deep networks used in feature extraction. In addition, a data augmentation operation is applied to increase the number of images in the dataset. The operations utilized in the augmentation process are presented in Tab. 3. The sample output of these operations is depicted in Fig. 7.

Table 3: Settings of image augmentation used in the proposed methodology

Operation	Value
Crop and Pad	0.25
Shear	16
Vertical Shift	0.2
Horizontal Shift	0.15
Rotation	45

Figure 7: Image augmentation results based on five transformations

5 Results and Discussion

The effectiveness of the proposed approach is validated in this section using a set of experiments based on the adopted dataset. The dataset images are split into training and testing sets. The training set is employed in terms of five-fold cross-validation to achieve better generalization and proper performance. Fig. 8 shows the cross-validation process. Each split in the five-fold cross-validation is used to train the proposed approach using four-folds, and the fifth fold is used for testing.

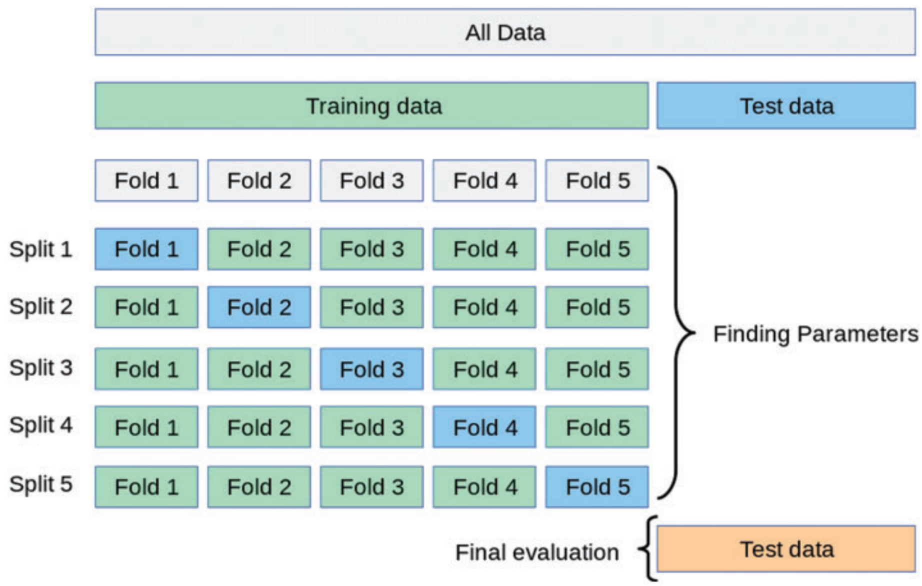

Figure 8: The five-fold cross-validation operation

5.1 Performance Measurement

A set of evaluation metrics were employed to measure the performance of the proposed approach. These metrics are positive predictive value, negative predictive value, accuracy, specificity, sensitivity, and F1-score. The measurement of these metrics is presented in Tab. 4.

5.2 Achieved Results

After extracting the main features using the three deep learning networks, namely, GoogLeNet, ResNet18, and DenseNet121, a set of experiments were conducted to find the best algorithm to be used for feature selection. Tab. 5 presents the results recorded by each of the binary optimization algorithms. From this table, it can be noted that the binary DTO achieves the best performance. Therefore, we adopted this algorithm for the feature selection in the proposed approach.

On the other hand, another set of experiments was implemented to measure the efficiency of three classifiers, namely, KNN, support vector machines (SVM), and random forest, using the selected features. Tab. 6 shows the results of the classification process in terms of the six evaluation criteria presented earlier. As shown in this table, the results achieved by the KNN classifier are the best among the three classifiers. Therefore, we adopted this classifier to classify the pneumonia cases in the proposed approach.

Table 4: Performance metrics

Metric	Value
Accuracy	$\frac{TP+TN}{TP+TN+FP+FN}$
Specificity	$\frac{TN}{TN+FP}$
Sensitivity	$\frac{TP}{TP+FN}$
Positive Predictive Value (PPV)	$\frac{TP}{TP+FP}$
Negative Predictive Value (NPV)	$\frac{TN}{TN+FN}$
F-score	$\frac{TP}{TP+0.5\,(FP+FN)}$

Table 5: The performance of the binary optimization algorithms

	bDTO	bGWO	bPSO	bBA	bWAO	bFA	bGA
Average error	0.7741	0.7913	0.8251	0.8347	0.8249	0.8235	0.8049
Average select size	0.7269	0.9269	0.9269	1.0663	1.0903	0.9614	0.8693
Average fitness	0.8373	0.8535	0.8519	0.8748	0.8597	0.9038	0.8649
Best fitness	0.7391	0.7738	0.8322	0.7645	0.8238	0.8225	0.7682
Worst fitness	0.8376	0.8407	0.8999	0.8661	0.8999	0.9201	0.8833
STD fitness	0.6596	0.6643	0.6637	0.6736	0.6659	0.7005	0.6659

Table 6: The performance of three classifiers on the pneumonia dataset

	KNN	SVM	Random forest
Accuracy	0.948717949	0.931034483	0.921568627
Sensitivity	0.925925926	0.874125874	0.833333333
Specificity	0.986394558	0.986394558	0.986394558
PPV	0.991189427	0.984251969	0.978260870
NPV	0.889570552	0.889570552	0.889570552
F-score	0.957446809	0.925925926	0.901201211

To achieve better classification results, a set of experiments were implemented to optimize the K parameter of the adopted KNN classification algorithm. Tab. 7 presents the performance of the optimized KNN using the continuous version of the optimizers used in feature selection. It can be noted from these results that KNN optimized using DTO (DTO + KNN) are better than the other optimizers. Therefore, this optimizer is recommended in the proposed approach. In addition, a more in-depth statistical analysis of the achieved results using the proposed approach with comparison to the other approaches is presented in terms of t-test and analysis of variance (ANOVA) test are presented in Tabs. 8 and 9.

Table 7: The performance of various optimizers for boosting the results of KNN

	DTO + KNN	WOA + KNN	GWO + KNN	GA + KNN	PSO + KNN
Number of values	14	14	14	14	14
Minimum	0.985	0.955	0.946	0.955	0.941
25% Percentile	0.988	0.965	0.956	0.975	0.961
Median	0.988	0.965	0.956	0.975	0.961
75% Percentile	0.988	0.965	0.956	0.975	0.961
Maximum	0.998	0.975	0.966	0.985	0.971
Range	0.013	0.020	0.020	0.030	0.030
10% Percentile	0.987	0.960	0.951	0.965	0.946
90% Percentile	0.998	0.970	0.966	0.980	0.966
Mean	0.9893	0.965	0.9567	0.9743	0.9596
Std. deviation	0.003791	0.003922	0.004746	0.006157	0.00663
Std. error of mean	0.001013	0.001048	0.001269	0.001646	0.001772
Coefficient of variation	0.3832%	0.4065%	0.4961%	0.6320%	0.6909%
Geometric mean	0.9893	0.965	0.9567	0.9743	0.9596
Geometric SD factor	1.004	1.004	1.005	1.006	1.007
Harmonic mean	0.9893	0.965	0.9567	0.9742	0.9595
Quadratic mean	0.9893	0.965	0.9567	0.9743	0.9596
Skewness	2.0150	0.000	0.3083	−2.283	−1.6970
Kurtosis	3.2070	6.500	2.9230	9.0600	5.1190
Sum	13.85	13.51	13.39	13.64	13.43

Table 8: Statistical t-test analysis of the results achieved by the optimized KNN and other approaches

	DTO + KNN	WOA + KNN	GWO + KNN	GA + KNN	PSO + KNN
Theoretical mean	0	0	0	0	0
Actual mean	0.9893	0.965	0.9567	0.9743	0.9596

(Continued)

Table 8: Continued

	DTO + KNN	WOA + KNN	GWO + KNN	GA + KNN	PSO + KNN
Number of values	14	14	14	14	14
One sample t test					
t, df	t = 976.3, df = 13	t = 920.6, df = 13	t = 754.2, df = 13	t = 592.1, df = 13	t = 541.5, df = 13
P value (two tailed)	<0.0001	<0.0001	<0.0001	<0.0001	<0.0001
P value summary	****	****	****	****	****
Significant (alpha = 0.05)?	Yes	Yes	Yes	Yes	Yes
How big is the discrepancy?					
Discrepancy	0.9893	0.965	0.9567	0.9743	0.9596
SD of discrepancy	0.003791	0.003922	0.004746	0.006157	0.00663
SEM of discrepancy	0.001013	0.001048	0.001269	0.001646	0.001772
95% confidence interval	0.987 to 0.992	0.963 to 0.967	0.954 to 0.960	0.971 to 0.978	0.956 to 0.9634
R squared (partial eta squared)	1	1	1	1	1

Table 9: Statistical ANOVA test of the achieved results using DTO + KNN

ANOVA table	SS	DF	MS	F (DFn, DFd)	*P* value
Treatment (between columns)	0.009734	4	0.002433	F (4, 65) = 90.70	$P < 0.0001$
Residual (within columns)	0.001744	65	0.00002683		
Total	0.01148	69			

Moreover, Fig. 9 depicts the histogram of the results achieved by the proposed approach and other competing approaches. These results show the stability of the proposed approach in classifying the pneumonia cases in the images of the test sets. On the other hand, the plots presented in Fig. 10 analyze the performance of the adapted DTO + KNN approach. As shown in these plots, the proposed approach could achieve promising classification results with reduced error rates that outperform the other approaches incorporated in the conducted experiments.

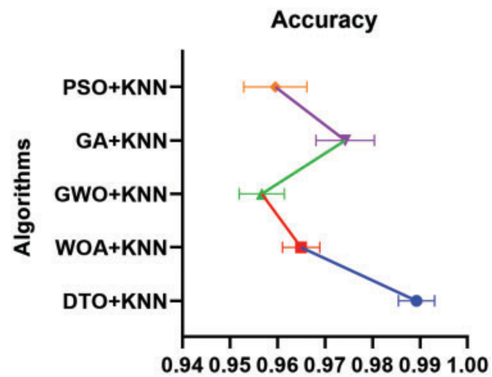

Figure 9: Histogram of the accuracy achieved by the proposed DTO + KNN and other approaches

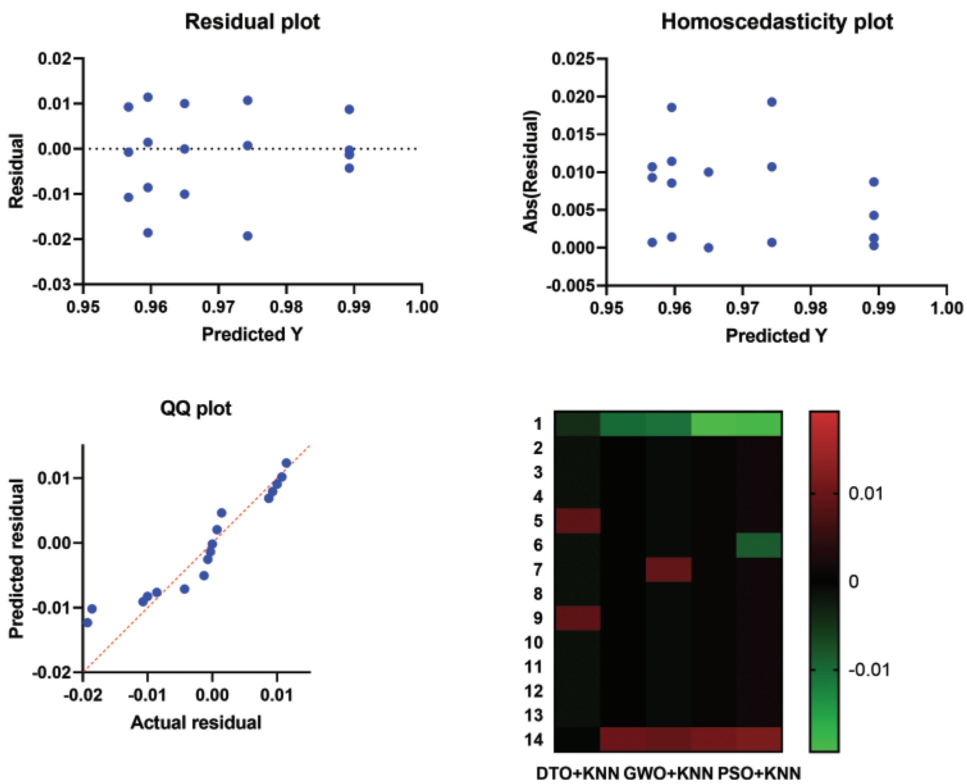

Figure 10: Homoscedasticity, residual, heat map, and QQ plots of the proposed approach

6 Conclusions and Future Perspectives

A novel approach is proposed in this paper for classifying the pneumonia cases based on deep learning for feature extraction and binary DTO for feature selection after preprocessing and augmenting the freely available Kaggle dataset. The selected features are used to train the KNN classifier using five-fold cross-validation. The proposed approach is evaluated in terms of several metrics and compared with other competing approaches in the literature. The recorded results emphasize the effectiveness of the proposed approach and its superiority. In addition, a set of experiments were conducted to analyze the achieved results statistically, and a set of plots were presented and discussed. The future perspectives of this work include the application of the proposed approach for classifying other types of lung diseases. In addition, the utilization of ensemble models can be considered a future work of the proposed approach.

Acknowledgement: Princess Nourah bint Abdulrahman University Researchers Supporting Project Number (PNURSP2022R308), Princess Nourah bint Abdulrahman University, Riyadh, Saudi Arabia.

Funding Statement: Princess Nourah bint Abdulrahman University Researchers Supporting Project Number (PNURSP2022R308), Princess Nourah bint Abdulrahman University, Riyadh, Saudi Arabia.

Conflicts of Interest: The authors declare that they have no conflicts of interest to report regarding the present study.

References

[1] T. Rahman, M. Chowdhury, A. Khandakar, K. Islam, K. Islam *et al.,* "Transfer learning with deep convolutional neural network (CNN) for pneumonia detection using chest X-ray," *Applied Sciences*, vol. 10, no. 1, pp. 3233, 2020.

[2] E. Ayan and H. Unver, "Diagnosis of pneumonia from chest X-ray images using deep learning," in *Proc. of the Scientific Meeting on Electrical-Electronics Biomedical Engineering and Computer Science (EBBT)*, Istanbul, Turkey, pp. 1–5, 2019.

[3] K. Nguyen, T. Son, T. Le, L. Tuan and T. Nguyen, "Applying multi-CNNs model for detecting abnormal problem on chest X-ray images," in *Proc. of the Int. Conf. on Knowledge and Systems Engineering (KSE)*, Ho Chi Minh City, Vietnam, pp. 300–305, 2018.

[4] G. Labhane, R. Pansare, S. Maheshwari, R. Tiwari and A. Shukla, "Detection of pediatric pneumonia from chest X-ray images using CNN and transfer learning," in *Proc. of the Int. Conf. on Emerging Technologies in Computer Engineering: Machine Learning and Internet of Things (ICETCE)*, Jaipur, India, pp. 85–92, 2020.

[5] O. Stephen, M. Sain, U. Maduh and D. Jeong, "An efficient deep learning approach to pneumonia classification in healthcare," *Journal of Healthcare Engineering*, vol. 2019, no. 1, pp. 4180949, 2019.

[6] A. Tahir, M. Chowdhury, A. Khandakar, S. Al-Hamouz, M. Abdalla *et al.,* "A systematic approach to the design and characterization of a smart insole for detecting vertical ground reaction force (vGRF) in gait analysis," *Sensors*, vol. 20, no. 1, pp. 957, 2020.

[7] M. Chowdhury, K. Alzoubi, A. Khandakar, R. Khallifa, R. Abouhasera *et al.,* "Wearable real-time heart attack detection and warning system to reduce road accidents," *Sensors*, vol. 19, no. 1, pp. 2780, 2019.

[8] M. Chowdhury, A. Khandakar, K. Alzoubi, S. Mansoor, A. Tahir *et al.,* "Real-time smart-digital stethoscope system for heart diseases monitoring," *Sensors*, vol. 19, no. 1, pp. 2781, 2019.

[9] K. Kallianos, J. Mongan, S. Antani, T. Henry, A. Taylor *et al.,* "How far have we come? Artificial intelligence for chest radiograph interpretation," *Clinical Radiology*, vol. 74, no. 1, pp. 338–345, 2019.

[10] V. Chouhan, S. Singh, A. Khamparia, D. Gupta, P. Tiwari *et al.,* "A novel transfer learning based approach for pneumonia detection in chest X-ray images," *Applied Sciences*, vol. 10, no. 1, pp. 559, 2020.

[11] J. Lujan-Garcia, C. Yanez-Marquez, Y. Villuendas-Rey and O. Camacho-Nieto, "A transfer learning method for pneumonia classification and visualization," *Applied Sciences*, vol. 10, no. 1, pp. 2908, 2020.

[12] A. Ibrahim, H. A. Ali, M. M. Eid and E. -S. M. El-Kenawy, "Chaotic harris hawks optimization for unconstrained function optimization," in *2020 16th Int. Computer Engineering Conf. (ICENCO)*, Cairo, Egypt, IEEE, pp. 153–158, 2020.

[13] S. S. M. Ghoneim, T. A. Farrag, A. A. Rashed, E. -S. M. El-Kenawy and A. Ibrahim, "Adaptive dynamic meta-heuristics for feature selection and classification in diagnostic accuracy of transformer faults," *IEEE Access*, vol. 9, pp. 78324–78340, 2021.

[14] M. M. Eid, E. -S. M. El-Kenawy and A. Ibrahim, "A binary sine cosine-modified whale optimization algorithm for feature selection," in *4th National Computing Colleges Conf. (NCCC 2021)*, Taif, Saudi Arabia, IEEE, pp. 1–6, 2021.

[15] A. A. Salamai, E. -S. M. El-kenawy, and A. Ibrahim, "Dynamic voting classifier for risk identification in supply chain 4.0," *Computers, Materials & Continua*, vol. 69, no. 3, pp. 3749–3766, 2021.

[16] E. -S. M. El-Kenawy, S. Mirjalili, S. S. M. Ghoneim, M. M. Eid, M. El-Said *et al.,* "Advanced ensemble model for solar radiation forecasting using sine cosine algorithm and newton's laws," *IEEE Access*, vol. 9, pp. 115750–115765, 2021.

[17] E. -S. M. El-kenawy, H. F. Abutarboush, A. W. Mohamed and A. Ibrahim, "Advance artificial intelligence technique for designing double T-shaped monopole antenna," *Computers, Materials & Continua*, vol. 69, no. 3, pp. 2983–2995, 2021.

[18] A. Ibrahim, S. Mirjalili, M. El-Said, S. S. M. Ghoneim, M. Al-Harthi *et al.,* "Wind speed ensemble forecasting based on deep learning using adaptive dynamic optimization algorithm," *IEEE Access*, vol. 9, pp. 125787–125804, 2021.

[19] E. -S. M. El-kenawy, A. Ibrahim, N. Bailek, K. Bouchouicha, M. A. Hassan *et al.,* "Sunshine duration measurements and predictions in Saharan Algeria region: An improved ensemble learning approach," *Theoretical and Applied Climatology*, vol. 2021, pp. 1–17, 2021.

[20] E. -S. M. El-kenawy, A. Ibrahim, N. Bailek, K. Bouchouicha, M. A. Hassan *et al.,* "Hybrid ensemble-learning approach for renewable energy resources evaluation in Algeria," *Computers, Materials & Continua*, vol. 71, no. 3, pp. 5837–5854, 2022.

[21] E. El-kenawy, A. Ibrahim, S. Mirjalili, Y. Zhang, S. Elnazer *et al.,* "Optimized ensemble algorithm for predicting metamaterial antenna parameters," *Computers, Materials & Continua*, vol. 71, no. 3, pp. 4989–5003, 2022.

[22] A. Ibrahim, H. Abutarboush, A. Mohamed, M. Fouad and E. El-kenawy, "An optimized ensemble model for prediction the bandwidth of metamaterial antenna," *Computers, Materials & Continua*, vol. 71, no. 1, pp. 199–213, 2022.

[23] E. -S. M. El-Kenawy, S. Mirjalili, A. Ibrahim, M. Alrahmawy, M. El-Said *et al.,* "Advanced meta-heuristics, convolutional neural networks, and feature selectors for efficient COVID-19 X-ray chest image classification," *IEEE Access*, vol. 9, pp. 36019–36037, 2021.

[24] E. -S. M. El-Kenawy, M. M. Eid, M. Saber and A. Ibrahim, "MbGWO-SFS: Modified binary grey wolf optimizer based on stochastic fractal search for feature selection," *IEEE Access*, vol. 8, pp. 107 635–107 649, 2020.

[25] E. S. M. El-Kenawy, A. Ibrahim, S. Mirjalili, M. M. Eid and S. E. Hussein, "Novel feature selection and voting classifier algorithms for COVID-19 classification in CT images," *IEEE Access*, vol. 8, pp. 179317–179335, 2020.

[26] Z. Xue, D. You, S. Candemir, S. Jaeger, S. Antani *et al.,* "Chest X-ray image view classification," in *Proc. of the IEEE 28th Int. Symp. on Computer-Based Medical Systems*, Sao Carlos, Brazil, pp. 66–71, 2015.

[27] D. Ragab, M. Sharkas, S. Marshall and J. Ren, "Breast cancer detection using deep convolutional neural networks and support vector machines," *PeerJ*, vol. 7, no. 1, pp. e6201, 2019.

[28] S. Pereira, A. Pinto, V. Alves and C. Silva, "Brain tumor segmentation using convolutional neural networks in MRI images," *IEEE Transactions on Medical Imaging*, vol. 35, no. 1, pp. 1240–1251, 2016.

[29] A. Esteva, B. Kuprel, R. Novoa, J. Ko, S. Swetter *et al.,* "Dermatologist-level classification of skin cancer with deep neural networks," *Nature*, vol. 542, no. 1, pp. 115–118, 2017.

[30] E. Ayan and H. Unver, "Data augmentation importance for classification of skin lesions via deep learning," in *Proc. of the 2018 Electric Electronics, Computer Science, Biomedical Engineering's Meeting (EBBT)*, Istanbul, Turkey, pp. 1–4, 2018.

[31] J. Ker, L. Wang, J. Rao and T. Lim, "Deep learning applications in medical image analysis," *IEEE Access*, vol. 6, pp. 9375–9389, 2017.

[32] G. Litjens, T. Kooi, B. Bejnordi, A. Setio, F. Ciompi *et al.,* "A survey on deep learning in medical image analysis," *Medical Image Analysis*, vol. 42, no. 1, pp. 60–88, 2017.

[33] H. Sak, A. Senior and F. Beaufays, “Long short-term memory recurrent neural network architectures for large scale acoustic modeling,” in *Proc. of the Annual Conf. of the Int. Speech Communication Association, INTERSPEECH*, Singapore, pp. 338–342, 2014.
[34] A. Gulli and S. Pal, *Deep Learning with Keras*, 1st ed., vol. 1, Birmingham, UK: Packt Publishing Ltd., 2017.
[35] E. Tsironi, P. Barros, C. Weber and S. Wermter, “An analysis of convolutional long short-term memory recurrent neural networks for gesture recognition,” *Neurocomputing*, vol. 268, pp. 76–86, 2017.
[36] P. Mooney, “Chest X-ray images (Pneumonia),” [Online]. Available https://www.kaggle.com/paultimothymooney/chest-xray-pneumonia (accessed on 10 March 2022). 2018.
[37] E. Bisong, *Building Machine Learning and Deep Learning Models on Google Cloud Platform*, New York, USA, Springer, Apress, pp. 59–64, 2019. [Online]. Available https://link.springer.com/book/10.1007/978-1-4842-4470-8.
[38] D. Ibrahim, “Deep-pneumonia framework using deep learning models based on chest X-ray images,” [Online]. Available https://github.com/Dr-Dina-M-Ibrahim/Pneumonia-Detection-using-Deep-Learning, 2018 (accessed on 10 February 2022).
[39] A. Takieldeen, E., El-kenawy, E. Hadwan and M. Zaki, “Dipper throated optimization algorithm for unconstrained function and feature selection,” *Computers, Materials & Continua*, vol. 72, no. 1, pp. 1465–1481, 2022.